Solid State Phenomena
ISSN: 1662-9779, Vol. 289, pp 127-133
doi:10.4028/www.scientific.net/SSP.289.127

Submitted: 2018-05-28
Revised: 2018-09-10
Accepted: 2018-09-10
Online: 2019-04-08

Disordered and Frustrated Magnetization in Coated $MnFe_2O_4$ Nanoparticles Prepared by Microwave Plasma Synthesis

K. Nadeem[1,a*], M. Kamran[1,b], H. Krenn[2, c], D. V. Szabo[3,d], U. Brossmann[4,e], and R. Würschum[4,f]

[1]Nanoscience and Technology Laboratory, International Islamic University, Islamabad, Pakistan

[2]Institute of Physics, Karl-Franzens University Graz, Universitätsplatz 5, A-8010 Graz, Austria

[3]Karlsruhe Institute of Technology, Institute for Applied Materials, 76344 Eggenstein-Leopoldshafen, Germany

[4]Institute of Materials Physics, University of Technology Graz, A-8010 Graz, Austria

[a]kashif.nadeem@iiu.edu.pk, [b]mkamran_18@yahoo.com, [c]heinz.krenn@uni-graz.at, [d]dorothee.szabo@kit.edu, [e]brossmann@tugraz.at, [f]wuerschum@tugraz.at

Keywords*:* Nanoparticles; Magnetic properties; Manganese ferrite; Coating; Spin glass

Abstract. Disordered and frustrated magnetization of different surface coated (Cr_2O_3, Co_3O_4, ZrO_2, and SiO_2) $MnFe_2O_4$ nanoparticles have been studied using SQUID-magnetometry. Magnetic measurements, such as ZFC/FC and ac-susceptibility evidence surface spin-glass behavior. ZFC/FC curves were also compared with numerical simulation to get information about effective anisotropy constants. Frequency dependent ac susceptibility results were analyzed by using Arrhenius, Vogel Fulcher and dynamic scaling laws to further confirm the spin-glass behavior. It is observed that the strength of surface spins disorder and frustration strongly depends upon the type of the coating material. All these analyses signify that disordered and frustrated surface magnetization in $MnFe_2O_4$ nanoparticles greatly depend on the type of the surface coating materials and are useful for controlling the nanoparticle's magnetism for different practical applications.

Introduction

Magnetic nanoparticles are promising candidates not only for technological applications but also for biological and medical applications due to their unique magnetic properties such as size dependent magnetization, high coercivity, soft magnetic nature and high Curie temperature [1]. Among these nanoparticles, manganese ferrite ($MnFe_2O_4$) is preferred due to greater biocompatibility and high magnetic susceptibility [2]. The magnetic properties of these nanoparticles can be tailored by two dominant features i.e. finite size and surface effects. Due to the smaller size, surface to volume ratio of the nanoparticles increases and the surface contribution to magnetization becomes significant. Atoms on the surface of these $MnFe_2O_4$ nanoparticles experience a different environment than those in the core. As a result, different types of defects can arise on the surface of these nanoparticles and these surface defects mainly depend on its nanoparticle's sizes. Aslibeiki *et al*. [3] investigated the formation of a disorder state at the surface of $MnFe_2O_4$ nanoparticles, showing lower magnetization than the bulk due to the size reduction.

The changes in the dynamic magnetic behavior due to surface disorder can be controlled by suitable surface coating [4]. The type of coating can affect the magnetic properties of the core and modify the interparticle dipolar interactions. Non-magnetic coating usually reduces the effective magnetization due to its non-magnetic nature and existence of canted spins, or spin glass like behavior [5]. Magnetic coating can generate efficient core-shell interface interactions which can modify the effective anisotropy due to interface coupling [6]. In this article, we have used different coatings on $MnFe_2O_4$ nanoparticles i.e. SiO_2 (non-magnetic), ZrO_2 (non-magnetic), Co_3O_4 (antiferromagnetic (AFM)) and Cr_2O_3 (AFM) to study the disordered and frustrated magnetization and compared their magnetic properties.

Experimental

Fig. 1 shows the schematic diagram for the preparation of coated $MnFe_2O_4$ nanoparticles by using the microwave plasma synthesis method [7]. For the synthesis of ZrO_2 coated nanoparticles, a 2.45 GHz microwave equipment with commercial components as microwave generator, magnetron, isolator, directional coupler and tri-stub-tuner (Muegge, Reichelsheim, Germany), and specially designed cavities, using the rotating TE_{11}-mode in consecutive arrangement were used. The diameter of the quartz glass reaction tube was 28 mm. The length of the plasma zone was 12 cm, which approximately corresponds to one wavelength λ of the 2.45 GHz microwaves. Initially, the precursors such as solid $Mn_2(CO)_{10}$ and liquid $Fe(CO)_5$ were mixed in the first zone for preparation of $MnFe_2O_4$ nanoparticles. The evaporated precursor is then carried through the plasma zone by using argon (Ar) as a carrier gas. A controlled amount of reaction gas (20% O_2 in Ar) is fed into the system just in front of the microwave discharge zone, in which the nanoparticles are formed. The second evaporation source is also used for nanoparticle surface coating and suitable precursors are used for coating of Cr_2O_3, Co_3O_4, SiO_2 and ZrO_2. The cooled glass-finger serves for the deposition of the nanoparticles as a dry powder. Finally, the cooled glass-finger is removed from the system and the nanoparticles can be collected in the form of dry powder.

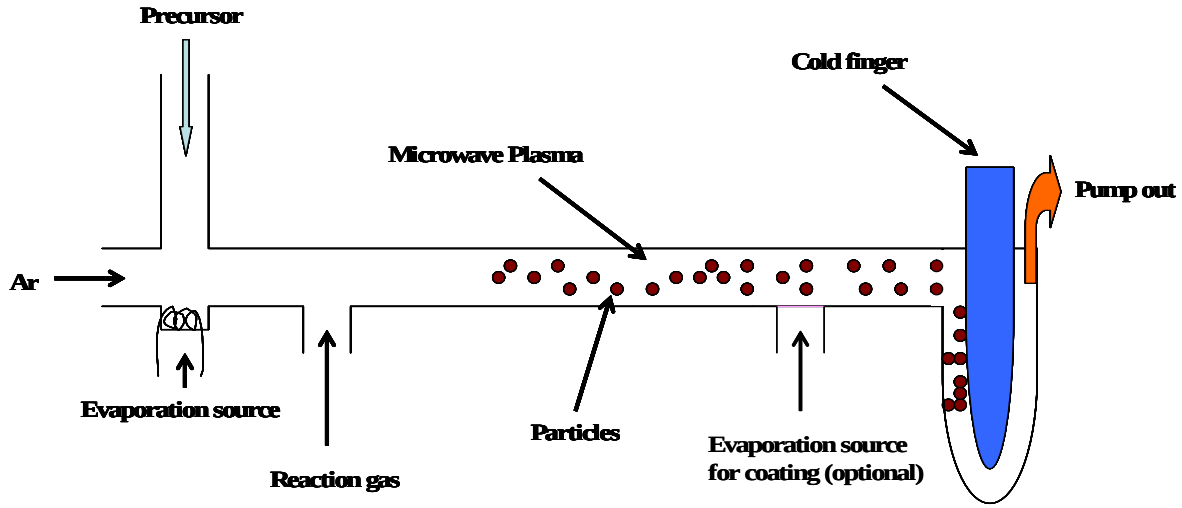

Fig. 1: Schematic diagram for the synthesis of coated $MnFe_2O_4$ nanoparticles.

Poly methyl methacrylate (PMMA) was further utilized as a protective layer for AFM Co_3O_4 and Cr_2O_3 coated nanoparticles. The inverse spinel structural phase was identified by X-ray diffraction (XRD) (Bruker D8 Advance instrument) by using Cu-Kα (λ=0.154nm) at ambient conditions. Transmission electron microscopy (TEM) was employed to analyze the shape and average particle size. Magnetic measurements were taken by using superconducting quantum interface device (SQUID) magnetometry (Quantum Design, MPMS-XL-7).

Results and Discussion

Fig. 2 (a-d) shows the XRD patterns of $MnFe_2O_4$ nanoparticles coated with Cr_2O_3, Co_3O_4, SiO_2 and ZrO_2, respectively.

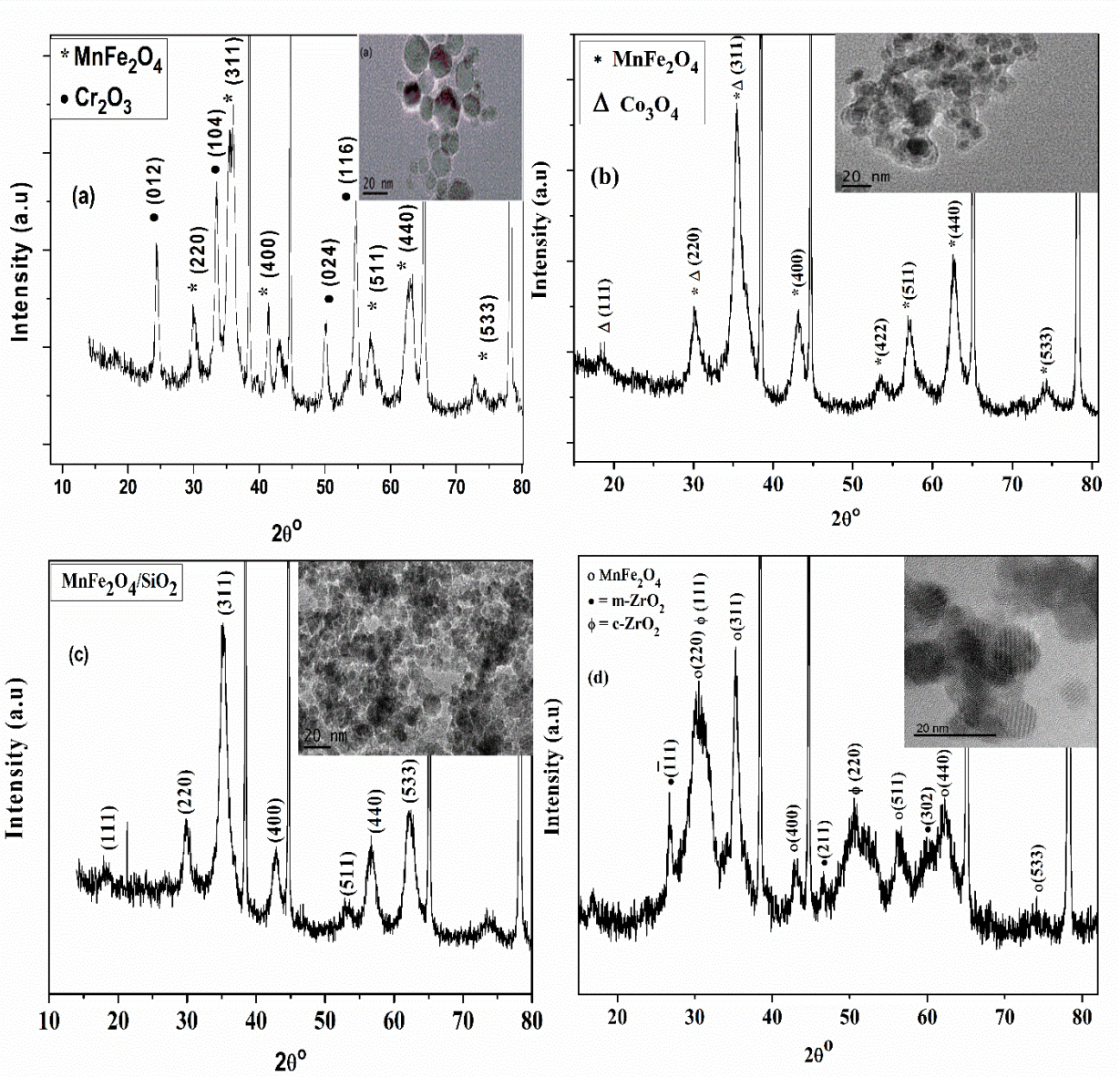

Fig. 2: (a) XRD patterns of Cr_2O_3, (b) Co_3O_4, (c) SiO_2 and (d) ZrO_2 coated $MnFe_2O_4$ nanoparticles. Insets show the TEM images at a 20 nm scale for respective nanoparticles samples.

All the indexed peaks matched very well the JCPDS card No. 10-0319 which represents the standard XRD pattern of $MnFe_2O_4$ nanoparticles. The peaks for $MnFe_2O_4$, Cr_2O_3, Co_3O_4, and ZrO_2 are identified as marks in the Fig. 2 (a-d). Very high intensity peaks, which are out of scale and also hidden by the insets, refer to the aluminum substrate. There are no peaks observed for SiO_2 due to its amorphous nature. The XRD average crystallite size (d_{XRD}) of these nanoparticles (by using Debye-Scherrer's formula) are tabulated in the Table 1. Insets in Fig. 2 (a-d) show the TEM images of Cr_2O_3, Co_3O_4, SiO_2 and ZrO_2 coated $MnFe_2O_4$ nanoparticles. These TEM images evidence a spherical shape of nanoparticles with less agglomeration.

Fig. 3 (a) shows experimental zero field cooled/field cooled (ZFC/FC) curves of Cr_2O_3, Co_3O_4, SiO_2 and ZrO_2 coated $MnFe_2O_4$ nanoparticles. In ZFC curve, at first the magnetization increases with increasing temperature due to the unblocking of particles and then decreases on further increasing of the temperature due to the onset of superparamagnetism. The broad maxima in the ZFC curve is the average blocking temperature (T_B) of the nanoparticles [8]. The Co_3O_4 coated

$MnFe_2O_4$ nanoparticles have higher T_B as compared to all other samples (see Table 1), which is attributed to enhanced magneto-crystalline anisotropy caused by Co_3O_4 surface coating [9,10]. Fig. 3 (b) shows experimental and simulated ZFC/FC curves of Cr_2O_3 coated $MnFe_2O_4$ nanoparticles. We have fitted our experimental ZFC/FC data by using Neel-Brown relaxation model [11]. It reveals a higher value of the effective anisotropy constant (K_{eff}) for all the samples as compared to their bulk value, K_{bulk} = 2.5x10^4 erg/cm^3 [12]. The surface anisotropy of $MnFe_2O_4$ nanoparticles is responsible for the increase of the K_{eff} value [12]. The Co_3O_4 coated nanoparticles show higher K_{eff} as compared to Cr_2O_3, SiO_2 and ZrO_2 coated $MnFe_2O_4$ nanoparticles (see Table 1) which is probably due to the AFM nature of the Co_3O_4 coating which gives rise to surface effects and enhanced surface/core-shell AFM/FM interface interactions. The large difference between the simulated and measured FC curves is attributed to our model limitations, because this model works only for non-interacting single-domain particles. The interacting nanoparticles usually show a plateau in the FC curve just below the T_B as evident from the flatness of the experimental FC curve below T_B as shown in Fig. 3 (b). Parameters obtained from the simulation of Cr_2O_3, Co_3O_4, SiO_2 and ZrO_2 coated $MnFe_2O_4$ nanoparticles are given in Table I.

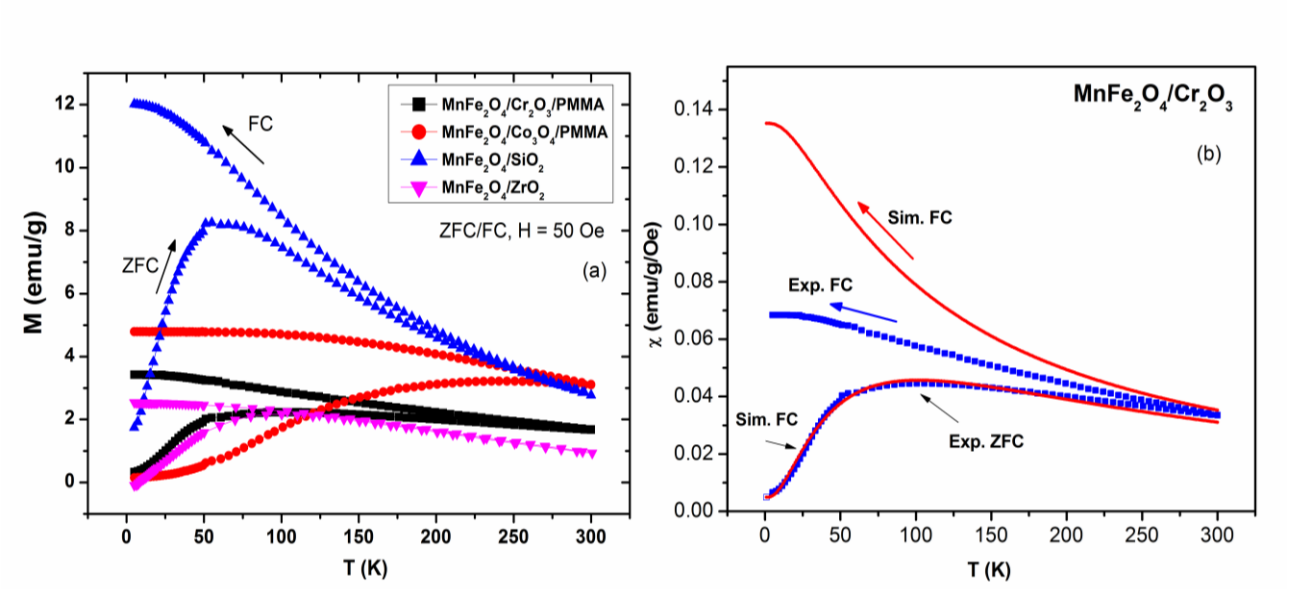

Fig. 3: (a) Experimental ZFC/FC curves of all the samples and **(b)** experimental and simulated ZFC/FC of Cr_2O_3 coated $MnFe_2O_4$ nanoparticles.

Table 1: Parameters obtained from experimental and simulated ZFC/FC curves and XRD analysis.

Samples	T_B [K]	K_{eff} [erg/cm^3]	M_S [emu/g]	d_{sim} [nm]	d_{XRD} [nm]	σ_D
$MnFe_2O_4/Cr_2O_3$	95	2 x 10^5	24.9	17	15-20	0.31
$MnFe_2O_4$/ Co_3O_4	238	5 x 10^6	38.6	6	7-10	0.22
$MnFe_2O_4/SiO_2$	65	9 x 10^5	39.7	6.6	8-10	0.25
$MnFe_2O_4/ZrO_2$	100	3 x 10^4	61.4	14.7	15-20	0.20

Disordered and frustrated surface spins freeze at lower temperatures and can give rise to spin-glass behavior. To investigate the spin-glass behavior in these nanoparticles, we carried out frequency dependent ac susceptibility measurements. Fig. 4 (a) shows the temperature dependent out-of-phase ac-susceptibility of Cr_2O_3 coated $MnFe_2O_4$ nanoparticles at frequencies (f) = 1, 10, 100 and 1000 Hz under magnetic field excitation with amplitude H_{ac} = 5 Oe. For the out-of-phase part, T_B is observed at 45, 55, 65 and 74 K at 1, 10, 100 and 1000 Hz frequency, respectively.

To confirm the existence of interparticle interactions and spin-glass behaviour, we have fitted the f-dependent shift of T_B for the out-of-phase ac-susceptibility by using different physical models. Neel-Arrhenius law is used for thermally non-interacting particles as shown in Fig. 4 (b). The

model is expressed as [13] $\tau = \tau_o e^{\left(\frac{E_a}{k_B T_B}\right)}$, where τ is the frequency dependent relaxation time of spins, E_a is activation energy barrier and τ_o is the atomic spin-flip time which lies in the range 10^{-9} to 10^{-12} s. The fitted parameters as obtained from Arrhenius law fit gives unreasonably large value for τ_o = 3.8x10^{-08} s. It shows that Cr_2O_3 coated nanoparticles do not obey the Neel-Arrhenius law and these nanoparticles are not completely non-interacting. SiO_2 and ZrO_2 coated $MnFe_2O_4$ nanoparticles nearly follow the thermally activated Neel-Arrhenius law and give reasonable values of τ_o which lies in or end of the range. In literature, it is mentioned that nanoparticles with $\tau_o = 10^{-13}$ s are considered as weakly interacting particles [14, 15]. Therefore there was no need of further investigation for these nanoparticles. The non-magnetic SiO_2 and ZrO_2 coating have minimized the surface energy and relaxed the surface spins of $MnFe_2O_4$ nanoparticles which are not able to create spin glass behaviour. Further analysis was done for Co_3O_4 and Cr_2O_3 coated $MnFe_2O_4$ nanoparticles. The Vogel–Fulcher law with an additional parameter T_o (interparticle interactions strength) can be written as [16], $\tau = \tau_o e^{\left(\frac{E_a}{k_B (T_B - T_o)}\right)}$. Fig. 4 (c) shows the best fit in terms of the Vogel-Fulcher law with reasonable values for the activation energy, E_a/k_B = 300 K, and τ_o = 1.7x10^{-12} s with a strength of interparticle interactions as T_o = 21 K. This value of T_o leads to moderate interparticle interactions for these nanoparticles.

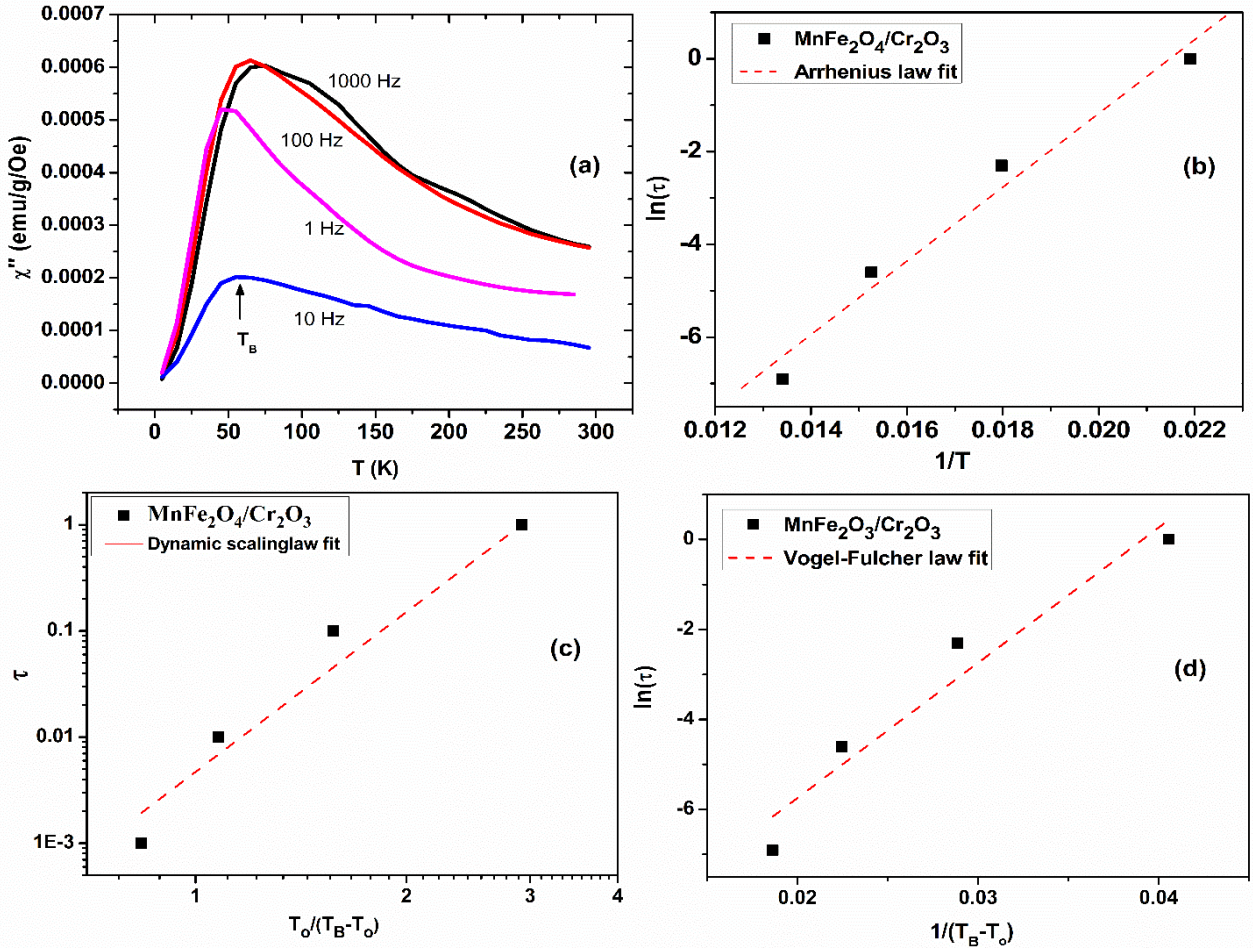

Fig. 4: (a) Out-of-phase ac-susceptibility measured at different frequencies (b) fit by an Arrhenius law, (c) fit by a Vogel-Fulcher law, and (d) fit by a dynamic scaling law.

For the study of spin glass behaviour, the dynamic scaling law is usually used, which can be expressed as [17] $\tau = \tau^* \left(\frac{T_o}{T_B - T_o} \right)^{zv}$, where τ^* is the spin-flip time for individual nanoparticle combined core spin, T_o is the static freezing temperature and "zv" is the critical exponent which gives information about the spin-glass behaviour, generally it ranges from 4 to 12 [18]. The obtained value of the spin flip time of nanoparticles as shown in Fig. 4 (d) is $\tau^* = 4.6 \times 10^{-03}$ s. Slow relaxation of frozen disordered surface spins and interparticle interactions are responsible for the higher value of τ^*. The critical exponent is 5 which lies in the spin-glass regime. We have also used the same physical models for other coated nanoparticles (not shown here) and obtained parameters, which are summarized in Table 2. The Co_3O_4 coated nanoparticles show higher value of activation energy and zv as compared to Cr_2O_3 coated nanoparticles [10]. The Co_3O_4 and Cr_2O_3 coated nanoparticles exhibit spin-glass behaviour, induced by disordered surface spins and interparticle interactions but with different strength and effective anisotropy, which is due to the two different coating material.

Table 2: Parameters obtained from different physical model fittings of the *f*-shift of T_B for $MnFe_2O_4$ nanoparticles coated with different materials.

Samples	Arrhenius law	Vogel-Fulcher law	Dynamic scaling law
$MnFe_2O_4/Co_3O_4$	$\tau_o = 4.3 \times 10^{-15}$ s $E_a/k_B = 4993.13$ K	$\tau_o = 4.56 \times 10^{-09}$ s $E_a/k_B = 1424$ K $T_o = 76$ K	$\tau^* = 7 \times 10^{-04}$ s $zv = 12$ $T_o = 80$ K
$MnFe_2O_4/ZrO_2$	$\tau_o = 1.2 \times 10^{-14}$ s $E_A/k_B = 3005$ K	- -	- -
$MnFe_2O_4/Cr_2O_3$	$\tau_o = 3.8 \times 10^{-08}$ s $E_a/k_B = 794.39$ K	$\tau_o = 1.7 \times 10^{-12}$ s $E_a/k_B = 300$ K $T_o = 21$ K	$\tau^* = 4.6 \times 10^{-03}$ s $zv = 5$ $T_o = 34$ K
$MnFe_2O_4/SiO_2$	$\tau_o = 4.6 \times 10^{-10}$ s $E_a/k_B = 987$ K	- -	- -

Conclusions

Surface spin disorder in $MnFe_2O_4$ nanoparticles coated with Cr_2O_3, Co_3O_4, SiO_2 and ZrO_2 was studied by ac and dc magnetization measurements. XRD confirmed the spinel crystal structure of $MnFe_2O_4$ nanoparticles and exhibit peaks for coating materials except for amorphous SiO_2. Experimental and simulated ZFC/FC curves revealed that the Co_3O_4 coated $MnFe_2O_4$ nanoparticles exhibit higher K_{eff} as compared to bulk MnF_2O_4 and higher T_B as compared to other coated nanoparticles. The higher value of K_{eff} is due to the AFM nature of Co_3O_4 surface coating which increases the core-shell interface interactions and surface disorder as compared to other coatings of the nanoparticles. The parameters obtained from model fittings showed that SiO_2 and ZrO_2 coated nanoparticles reduced surface disorder and frustration. However, Co_3O_4 and Cr_2O_3 coated nanoparticles exhibited spin-glass behaviour but with different interaction strength parameters. All these findings demonstrate that surface spins disorder and frustration can be modified by using suitable coating material for desired applications.

Acknowledgment

K. Nadeem acknowledges the Higher Education Commission (HEC) of Pakistan for providing research funds.

References

[1] S. Bedanta and W. Kleemann, Supermagnetism, J Phys. D. Appl. Phys., 42 (2008) 013001.

[2] D.-H. Kim, D.E. Nikles and C.S. Brazel, Synthesis and Characterization of Multifunctional Chitosan-$MnFe_2O_4$ Nanoparticles for Magnetic Hyperthermia and Drug Delivery, Materials 3 (2010) 4051-4065.

[3] B. Aslibeiki, P. Kameli, H. Salamati, M. Eshraghi and T. Tahmasebi, Superspin Glass State in $MnFe_2O_4$ Nanoparticles, J. Magn. Magn. Mater., 322 (2010) 2929-2934.

[4] J. Jorzick, C. Krämer, S. Demokritov, B. Hillebrands, B. Bartenlian, C. Chappert, D. Decanini, F. Rousseaux, E. Cambril and E. So/ndergard, Spin Wave Quantization in Laterally Confined Magnetic Structures, J. Appl. Phys., 89 (2001) 7091-7095.

[5] R. Kodama, Magnetic Nanoparticles, J. Magn. Magn. Mater., 200 (1999) 359-372.

[6] C.C. Berry and A.S. Curtis, Functionalisation of Magnetic Nanoparticles for Applications in Biomedicine, J. Phys. D. Appl. Phys., 36 (2003) R198.

[7] D. Vollath and D.V. Szabó, The Microwave Plasma Process–a Versatile Process to Synthesise Nanoparticulate Materials, J. Nanopart. Res., 8 (2006) 417-428.

[8] B.D. Cullity and C.D. Graham, Introduction to Magnetic Materials, John Wiley & Sons, 2011.

[9] A. Ślawska-Waniewska, P. Didukh, J. Greneche and P. Fannin, Mössbauer and Magnetisation Studies of $CoFe_2O_4$ Particles in a Magnetic Fluid, J. Magn. Magn. Mater., 215 (2000) 227-230.

[10] F. Zeb, M. Ishaque, K. Nadeem, M. Kamran, H. Krenn, D. V. Szabó'. Surface Effects and

Spin Glass State in Co_3O_4 Coated $MnFe_2O_4$ Nanoparticles, Mater. Res. Express, 5 (2018) 086109.

[11] J. Denardin, A. Brandl, M. Knobel, P. Panissod, A. Pakhomov, H. Liu and X. Zhang, Thermoremanence and Zero-Field-Cooled/Field-Cooled Magnetization Study of $Co_x(SiO_2)_{1-x}$ Granular Films, Phys. Rev. B, 65 (2002) 064422.

[12] S. Yoon and K.M. Krishnan, Temperature Dependence of Magnetic Anisotropy Constant in Manganese Ferrite Nanoparticles at Low Temperature, J. Appl. Phys., 109 (2011) 07B534.

[13] L. Néel, Théorie Du Traînage Magnétique De Diffusion, J. Phys. Radium 13 (1952) 249-264.

[14] S. H. Masunaga, R. d. F. Jardim, P. F. P. Fichtner, J. Rivas, Role of Dipolar Interactions in a System of Ni Nanoparticles Studied by Magnetic Susceptibility Measurements, Phys. Rev. B 80 (2009) 184428.

[15] C. Cannas, G. Concas, D. Gatteschi, A. Falqui, A. Musinu, G. Piccaluga, C. Sangregorio, G. Spano, Superparamagnetic Behaviour of γ-Fe_2O_3 Nanoparticles Dispersed in a Silica Matrix, Phys. Chem. Chem. Phys., 3 (2001) 832-838.

[16] J. Dormann, D. Firorani and E. Tronc, Magnetic Relaxation in Fine Particle Systems, Advances in Chemical Physics, John Wiley & Sons, Inc., New York (1997).

[17] D. Kumar and A. Banerjee, Coexistence of Interacting Ferromagnetic Clusters and Small Antiferromagnetic Clusters in $La_{0.5}Ba_{0.5}CoO_3$, J. Phys. Condens. Matter, 25 (2013) 216005.

[18] S. He, J.S. DuChene, J. Qiu, A.A. Puretzky, Z. Gai and W.D. Wei, Persistent Photomagnetism in Superparamagnetic Iron Oxide Nanoparticles, Adv. Electron Mater., 4 (2018) 1700661.